Periodic negative differential conductance in a single metallic nanocage

Yehonadav Bekenstein,[1,2] Kathy Vinokurov,[2] Tal J. Levy,[3] Eran Rabani,[3,*] Uri Banin,[2,*] and Oded Millo[1,*]

[1]*Racah Institute of Physics and the Center for Nanoscience and Nanotechnology, The Hebrew University of Jerusalem, Jerusalem 91904, Israel*

[2]*Institutes of Chemistry and the Center for Nanoscience and Nanotechnology, The Hebrew University of Jerusalem, Jerusalem 91904, Israel*

[3]*School of Chemistry, Sackler Faculty of Exact Sciences, Tel Aviv University, Tel Aviv 69978, Israel*

(Received 22 March 2012; published 17 August 2012)

We report a bipolar multiple periodic negative differential conductance (NDC) effect on a single cage-shaped Ru nanoparticle measured using scanning tunneling spectroscopy. This phenomenon is assigned to the unique multiply connected cage architecture providing two (or more) defined routes for charge flow through the cage. This, in turn, promotes a self-gating effect, where electron charging of one route affects charge transport along a neighboring channel, yielding a series of periodic NDC peaks. This picture is established and analyzed here by a theoretical model.

DOI: 10.1103/PhysRevB.86.085431 PACS number(s): 73.63.Kv, 73.23.Hk

Multiple negative differential conductance (NDC),[1–3] in which increase in voltage leads to decrease in current at several consecutive voltage values, has been reported previously for resonant tunneling-diode devices based on semiconductor heterostructures.[4,5] The multiple NDC effect was utilized in functional electronic devices to realize multiple value logic, ultra-high speed analog-to-digital converters, frequency multipliers, and other circuit elements.[6,7] However, these devices require relatively complex fabrication with characteristic micron-scale dimensions and typically exhibit only 2–4 nonperiodic NDC peaks for one bias polarity. It is of interest to reduce the device size, on one hand, and obtain a bipolar multiple periodic NDC effect, on the other hand. This was discovered by us for single empty Ru nanocages, where the tunneling I-V (current-voltage) characteristics measured using scanning tunneling spectroscopy (STS) exhibit up to six periodic NDC peaks, for both bias polarities. As shown below, quite frequently the expected conventional Coulomb staircase effect[8] measured on an Ru nanocage surprisingly evolved into a series of NDC peaks, while nearly maintaining the staircase periodicity (as a function of bias). As demonstrated by a model simulation, this intriguing phenomenon is well accounted for by the unique multiply connected cage architecture, which enables a self-gating-like effect between neighboring transport channels through the different cage arms.

We study here Ru nanocages, whose discovery was reported by us recently.[9,10] These are synthesized starting from a hybrid semiconductor/metal quantum dot (QD) comprising a metallic Ru cagelike shell grown selectively on the edges of a semiconducting Cu_2S nanocrystal. The empty Ru cages were then obtained by methanol addition to a solution of Cu_2S/Ru hybrids in toluene, leading to selective dissolution of the Cu_2S from the cage interior.

To study the electronic and transport properties of this system, we utilized scanning tunneling microscopy (STM) and STS. These are effective tools for studying the electrical properties of nanostructured systems. They are particularly suitable for hybrid and cagelike QDs due to the ability of measuring the local density of states (DOS) with nanometric spatial resolution.[11–14] For the STM measurements, QD solutions were drop cast onto a flame-annealed Au(111) substrate and let dry (Fig. S1 in the supplementary material).[15] The STM measurements were performed at 4.2 K, using Pt-Ir tips, in clean He exchange gas inserted into the sample space after evacuation. Tunneling current-voltage (I-V) characteristics were acquired after positioning the STM tip at different locations above individual QDs, realizing a double barrier tunnel junction (DBTJ) configuration,[8] and disabling momentarily the feedback loop. The dI/dV-V tunneling spectra were numerically derived from the measured I-V curves. The topographic images were acquired with current and sample-bias set values of $I_s \cong 0.1$ nA and $V_s \cong 1$ V. Here, 20 Ru cages were measured, out of which eight showed periodic NDC effect. No such effect was found on any of the 10 Cu_2S/Ru hybrids that were measured, which exhibited only the conventional single electron tunneling (SET) behavior (on the Ru cage).

The STM images of single Ru cages having two different orientations deposited on a conducting Au(111) substrate (supplementary material Fig. S1)[15] along with the corresponding scanning transmission electron microscope (STEM) images and illustrations are presented in Figs. 1(a)–1(f). The two different projections demonstrate the cage structure, depicting the median arm and the pore of the cage. Figure 1 also presents I-V characteristics and the corresponding dI/dV-V spectra acquired on the Ru cage (inset). The blue (medium gray) curves exhibit conventional SET effects,[16,17] the Coulomb blockade, and staircase, commonly observed in tunneling through metallic nanostructures.[8] The former manifests itself in the suppression of the tunneling current and the DOS around zero bias, while the latter by a periodic series of broadened steps (peaks) in the I-V (dI/dV-V) characteristics, each corresponding to the addition of a single electron to the Ru cage. Surprisingly, however, in many cases, we observed a set of periodic NDC peaks, as shown by the green (gray) curves. We have verified that the oscillation period, as a function of bias, was independent of the bias sweep rate over a very wide range, 10 to 500 V/s, thus ruling out the possibility that these features are associated with pick-up of external noise. The I-V curves on a given cage showed, in different scans, either the conventional Coulomb blockade and staircase behavior (blue [medium gray] curves) or the periodic NDC

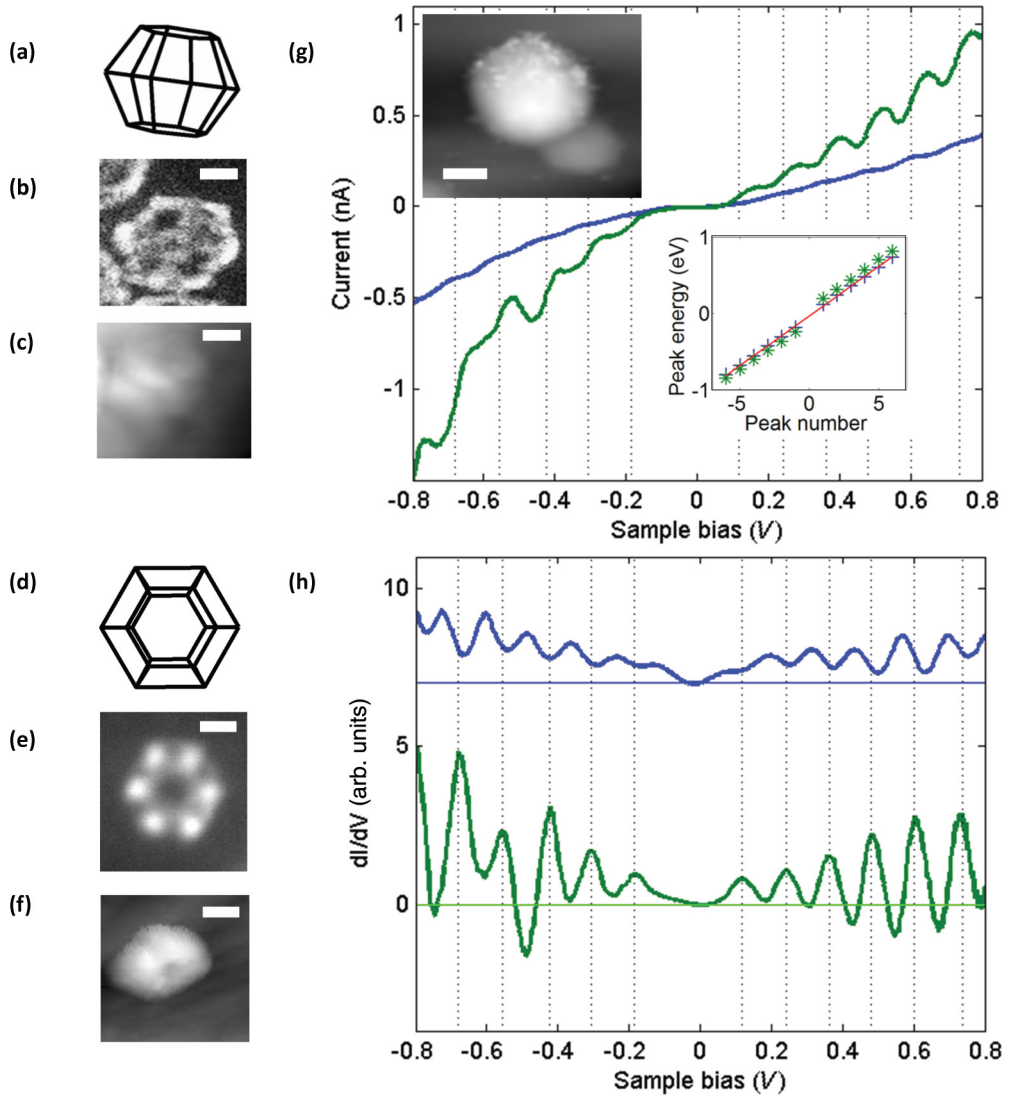

FIG. 1. (Color online) STS measurements on an empty Ru cage revealing negative tunneling conductance. (a)–(f) Illustrations, STEM and STM images portraying two different projections of the Ru cage, one is emphasizing (a)–(c) the median arm, and the other (d)–(f) the pore of the cage. Scale bars for the (b) and (e) STEM and (c), (f), and (g inset) STM images are 5 nm. The grayscale range in the STM images is 0–5 nm. (g) I-V curves and (h) corresponding dI/dV-V tunneling spectra, offset vertically for clarity, measured at 4.2 K on the same Ru cage, portraying Coulomb staircase (blue [medium gray] curves) and the NDC effect (green [gray] curves). Evidently, the staircase charging peaks correlate well with the NDC features. The green and blue spectra were measured at the same bias and current set-points, $V_s = 0.172$ V and $I_s = 49.6$ pA. The lower inset of (g) presents the peak bias values (for both sets) as a function of peak number (negative for negative bias values).

effect (green [gray] curves), while roughly maintaining the same periodicity, pointing to a connection between the two phenomena. The transition between the staircase and NDC behaviors was accompanied by a change (increase or decrease) of the overall tunneling resistance.

The inset of Fig. 2(g) depicts the bias values of the peaks of the dI/dV-V curves for both NDC and SET (staircase) data [seen in Figs. 1(g) and 1(h)] as a function of peak number (negative for negative bias values). In the SET case, it is well established that each peak is due to a change by one in the number of excess electrons on the cage, and the average single electron charging energy can be readily extracted from this plot $U \sim 130$ meV. Using the simplistic formula $U = e^2/2C$, an average effective capacitance of $C = 6.2 \times 10^{-19} F$ is obtained for this tip-QD-substrate configuration, while fit to the orthodox model[8] for SET yields comparable values for the tip-cage and cage-substrate junction capacitances, $C_1 = 4 \times 10^{-19} F$ and $C_2 = 13 \times 10^{-19} F$, respectively (supplementary material Fig. S11)[15] Remarkably, the peak spacing in the NDC case nearly coincides with that of the staircase, indicating that the underlying NDC mechanism must be associated with single electron charging of the cage. Note, however, that there is a small shift between the two sets of peaks, a point that is addressed below. The single electron charging energies measured on all the empty Ru nanocages largely varied from one QD to another, between ~100 to ~300 meV, as shown by supplementary material Fig. S12,[15] yet in all cases where NDC peaks emerged, their periodicity corresponded well to

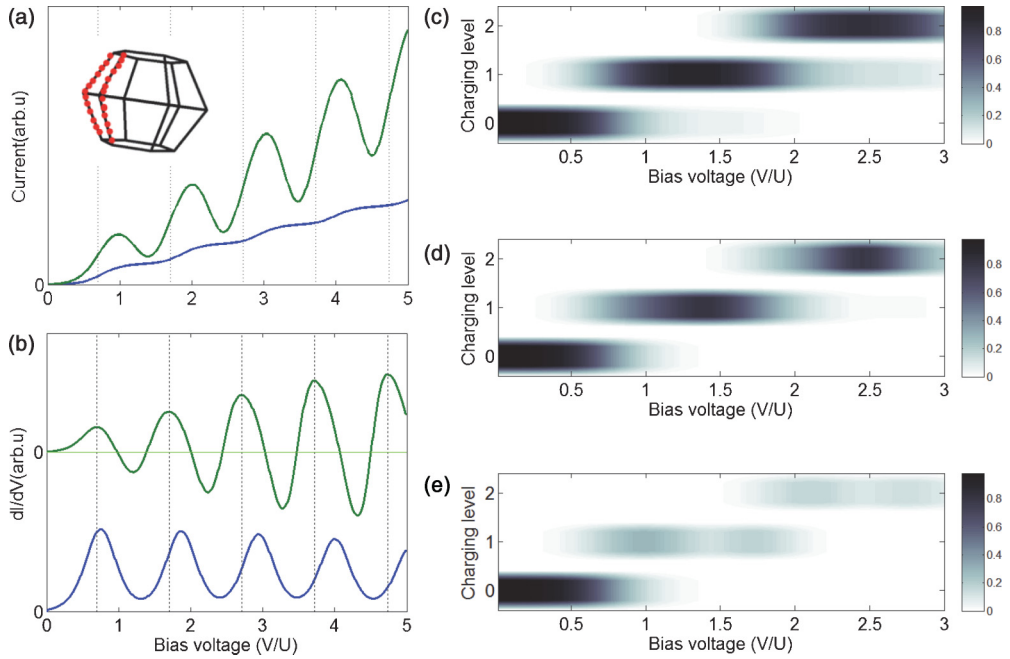

FIG. 2. (Color online) (a) Simulated I-V curves and (b) corresponding dI/dV-V curves calculated using a master equation approach as described in the text. The sample bias V is normalized to the single electron charging energy U. The inset of (a) depicts the Ru-cage geometry, where the two coupled active conduction channels are drawn in red. In the case where the two coupled channels are both connected to the substrate and STM tip with similar tunneling resistances, we observe a periodic Coulomb staircase with spacing $\sim U$ (blue [medium gray] curves). When one of the channels is effectively disconnected from either the STM tip or the substrate, periodic NDC emerges (green [gray] curves). (c) The charging level occupation diagram for the case where both channels are equally coupled to the tip and the substrate and conventional SET characteristics are observed. (d)–(e) The case where NDC is observed; (d) showing the level occupation of the disconnected cannel and (e) of the conducting one.

the staircase periodicity, as in the cases depicted by Fig. 1 and supplementary material Fig. S13.[15] This large spread in charging energies may be attributed mainly to variations in the tunnel junction parameters between measurements and also to the spread in the widths of the arms between nanocages, but not solely to variations in their diameters that have a rather narrow size distribution of less than 13% (supplementary material Fig. S12).[15]

The NDC effects have been observed previously in resonant tunneling diodes made of micron-sized semiconductor heterostructures[2,3] and on various DBTJ configurations, either lithographically defined in two-dimensional electron gas[18] or achieved, as in our case here, in STS measurements of QDs.[11,19] However, bipolar periodic NDC oscillations correlated with the Coulomb staircase, as well as the bistability between SET and NDC behavior, have not yet been reported. The origin of the periodic NDC is attributed to the special multiply connected geometry of the empty-cage QD, providing multiple defined routes for charge flow through the cage. This, in turn, may promote a self-gating-like effect, where electron charging of one route may influence current flow through neighboring routes,[20,21] yielding a series of NDC peaks with the Coulomb staircase periodicity as a function of bias voltage.

To study this conjecture, we devised a simplified model[17,22] that considers two coupled conducting channels provided by the Ru cage, each supporting several charging levels. The two channels are also connected by tunneling barriers (i.e. weakly coupled) to the STM tip and the conducting substrate. A model Hamiltonian describing the electronic structure of the Ru cage is given by:

$$H_{\text{cage}} = \varepsilon \sum_{\nu=\alpha,\beta} \sum_{i} n_i^{\nu} + U \sum_{\nu=\alpha,\beta} \sum_{i>j} n_i^{\nu} n_j^{\nu} + U_{\text{int}} \sum_{i,j} n_i^{\alpha} n_j^{\beta}.$$

The first term in H_{cage} represents the noninteracting energy for each state i on the two channels $\nu = \alpha, \beta$, which also models the effects of the Fermi level offset affecting the Coulomb blockade. The second term represents the sum of charging energies (U) of the two individual channels, where $n_i^{\nu} = 1$ or 0 if state i on channel ν is occupied by an electron or not, respectively. This term provides the Coulomb staircase in the case of uncoupled channels. The third term represents the interaction energy (U_{int}) between the two channels on the cage.

Figures 2(a) and 2(b) show simulated I-V and dI/dV-V curves calculated using a master equation approach[23] for the above model (see supplementary material for more details).[24] First, we consider the case where the two coupled channels are both connected to the substrate and STM tip with similar tunneling resistances. In this case (blue [medium gray] curves), we observe a periodic Coulomb staircase with spacing $\sim U$ (for simplicity we take U in units of Volts). This equal spacing arises because of the identical charging energies assigned to both channels in the model and choosing U_{int} to be comparable to U, while nonequidistant Coulomb steps are obtained when the charging energies differ significantly (not shown). Importantly, NDC is not observed, irrespective of the relative magnitudes of U and U_{int} (supplementary material

Fig. S3).[24] Therefore, coupling between the channels by itself does not lead to NDC.

The NDC emerges when one of the channels is effectively disconnected from either the STM tip or the substrate (but not from both) and U_{int} is sufficiently large ($U_{\text{int}} > 0.6U$) to reduce the current through the conducting channel (supplementary material Fig. S4).[24] Such large values of U_{int} are expected, based on classical electrostatics, when the separation between the arms is smaller than $5R$, where R is the radius of the arms (supplementary material Fig. S9),[24] a condition that is satisfied in our cages, at least near junctions between neighboring arms. Here, I-V and dI/dV-V characteristics for this case are shown in Figs. 2(a) and 2(b), respectively (green [gray] curves). The observed NDC, which is consistent with the experiments, can be traced to a local gating-like effect of the blocked channel on the conducting one. While practically only the fully connected channel contributes to the current, both channels can be charged, as portrayed by the charging level occupation diagrams in Figs. 2(d) and 2(e) for the blocked and conducting channels, respectively. When the bias voltage increases towards U, both channels are partially charged, and the current increases. Increasing the bias voltage above U leads initially to a decrease in the total current since the charge on the blocked channel increases, hampering conduction through the open channel due to the Coulomb repulsion. Further increase of the bias voltage opens higher charging levels for conduction, and the current increases again while the second charging level of both channels start to populate, reaching a maximum at $V \sim 2U$. Above this bias, the blocked channel is further charged, decreasing again the current in the conducting channel via Coulomb repulsion. The above NDC mechanism repeats itself at bias values with periodicity U, with the periodicity arising from consecutive single electron (or hole) charging events in the coupled channels. This mechanism is similar in spirit to NDC induced by populations switching in SET of coupled QDs,[11,18,25] where the charging level of the blocked channel increases [Fig. 2(d))] at the account of that of the conducing channel [Fig. 2(e)]. However, while in previous studies only a single event of population switching was observed, the present case gives rise to multiple periodic events, taking place both at positive and negative bias values.

This model captures the essence of transport through the unique multiply connected cage structure and indeed accounts for the observed experimental data. First, the experimental curves showing the NDC (green [gray] curves, Fig. 1) have approximately the Coulomb staircase periodicity (blue [medium gray] curves), fully consistent with the model (see supplementary material section II for more details).[24] The high symmetry of the cage structure can indeed lead to appearance of two parallel channels with similar charging energies, as assumed in the model. Furthermore, the different pathways of conductance in the cage may be disconnected from one another while they are still coupled electrostatically. Indeed, structural analysis with STEM and TEM tomography shows disconnections in the polycrystalline Ru cages.[9] The transition between conventional SET to NDC in the experiments may be attributed to reorientation of the cage or to slight movement of the tip along the nanocage. This, in turn, can lead to the situation where tunneling resistance in the junction between one of the channels to one lead, most likely the tip, becomes much larger than all others, leading to effective blocking of the current through that channel.

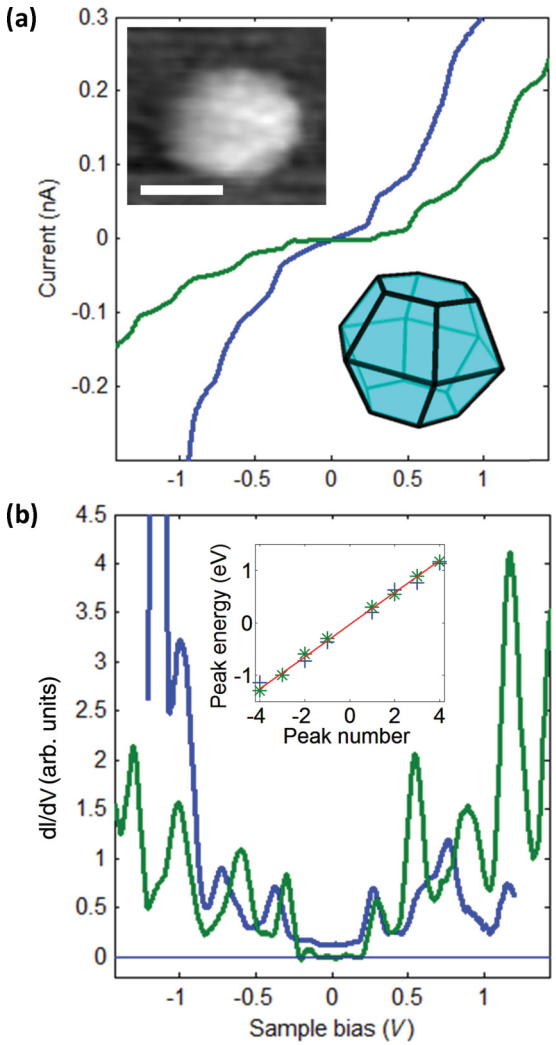

FIG. 3. (Color online) (a) I-V and (b) corresponding dI/dV-V tunneling spectra measured at 4.2 K on the Ru cage encapsulating the CU_2S core of a hybrid Cu_2S/Ru-cage QD [that is illustrated in the inset of (a)]. The spectra manifest SET effects typical for metallic dots, the Coulomb blockade and staircase. The green and blue spectra were measured with different bias and current set-point ($V_s = 0.94$ V and 0.74 V and $I_s = 65$ and 78 pA, respectively), thus affecting the tip-cage distance and consequently the value of the residual offset charge, suppressing the blockade (supplementary material Fig. S10).[15] The periodicity of the staircase was only slightly affected. (a) top inset: depicts an STM images portraying a Cu_2S/Ru cage. Scale bar for the STM image is 5 nm and the grayscale range is 0–5 nm. The inset of (b) presents the conductance-peak bias values plotted as a function of peak number (negative for negative bias values) for the two curves, in corresponding colors. The voltage differences between adjacent peaks are presented in supplementary material Fig. S12.[15]

A more subtle observation that nevertheless requires attention is the small shift between the peaks of the NDC and Coulomb staircase spectra, seen in both experimental and theoretical curves. The shifts result mainly from changes in the junction parameters taking place due to the aforementioned tip movement and/or QD reorientation that lead to the switching

between the conventional SET and NDC behaviors. These, in turn, yield small changes in the charging energy and effective residual charge Q_0,[8] as well as in the coupling strengths to the external electrodes. The theoretical curve presented in Fig. 2 was calculated considering only the latter effect, giving rise to an opposite shift compared to that in the experimental curve shown in Fig. 1. Additional experimental spectra, showing other (either positive or negative) shifts between the NDC and SET peaks, along with corresponding theoretical curves, are presented in supplementary material Fig. S13.[15]

Further insight and support for the periodic NDC mechanism suggested above is provided by the STS results measured on the hybrid Cu_2S/Ru-cage QD (before leaching out the Cu_2S core). When positioning the tip on the surrounding Ru cage, tunneling spectra manifesting SET effects were observed, as shown by Fig. 3 for two different bias and current settings. Changing the STM settings affects the tip-QD distance and the corresponding junction capacitance,[26] consequently generating a gating-like effect by changing Q_0[8,27] (see supplementary material section IV).[15] Indeed, the zero-bias gap in the tunneling spectrum presented by the green (gray) curves vanished upon modifying the STM setting, taken over by a linear I-V behavior at low bias [Fig. 3(a), blue (medium gray) curves]. This behavior, a hallmark of SET effect, establishes that the gap in the former spectrum is due to the Coulomb blockade.[8] At higher bias, both spectra show a Coulomb staircase behavior with similar period of $\sim$315 meV (inset of Fig. 3). This is the largest charging energy observed for the hybrids, whereas the lowest observed value was $\sim$140 meV (supplementary material Fig. S12).[15] We note in passing that the STS data on the hybrids taken at other positions showed different behaviors, manifesting significantly larger gaps of up to 1.4 eV, corresponding to the band gap of the semiconducting Cu_2S core decorated by in-gap states (discussed elsewhere). Importantly, NDC effects were not observed for the hybrid QD irrespective of the STM settings. This is consistent with the hybrid structure that supports and reinforces the external metallic cage structure grown onto it, thus minimizing the possibility of disconnected routes. Additionally, the Cu_2S core can electrically bypass possible disconnections in the Ru cage and also reduce U_{int} by screening the electrostatic coupling between the channels (supplementary material Fig. S6).[15]

In summary, we observed a bipolar multiple periodic NDC effect on a single cage-shaped Ru nanoparticle using scanning tunneling spectroscopy. A simple model was developed, relating this effect to the unique multiply connected cage architecture which promotes a self-gating effect, where electron charging of one disconnected route has an effect on a neighboring channel, yielding a series of periodic NDC peaks. This mechanism is expected to be generic and applicable to other types of nanoscale multiply connected systems that can thus be designed to exhibit multiple NDC with requested periodicity, opening a gateway for the construction of nanoscale electronic devices utilizing this unique effect.

The research received funding from the ERC, FP7 Grant Agreement No. [246841] (U.B.), the ISF (O.M.), the US-Israel BSF (E.R.), and the FP7 Marie Curie IOF project HJSC (E.R). T.J.L. thanks the Nano-Center at Tel Aviv University for a doctoral fellowship. We are grateful to Eran Socher and Avraham Schiller for helpful discussions.

*To whom correspondence should be addressed: rabani@tau.ac.il; uri.banin@huji.ac.il; milode@vms.huji.ac.il

[1] L. Esaki, Phys. Rev. **109**, 603 (1958).
[2] L. Esaki and R. Tsu, IBM J. Res. Dev. **14**, 61 (1970).
[3] L. Esaki and L. L. Chang, Phys. Rev. Lett. **33**, 495 (1974).
[4] K. K. Choi, B. F. Levine, R. J. Malik, J. Walker, and C. G. Bethea, Phys. Rev. B **35**, 4172 (1987).
[5] W. C. Liu, H. J. Pan, W. C. Wang, S. C. Feng, K. W. Lin, K. H. Yu, and L. W. Laih, IEEE Trans. Electron Devices **48**, 1054 (2001).
[6] S. Sen, F. Capasso, A. Y. Cho, and D. Sivco, IEEE Trans. Electron Devices **34**, 2185 (1987).
[7] S. Sen, F. Capasso, A. Y. Cho, and D. L. Sivco, IEEE Electron Device Lett. **9**, 533 (1988).
[8] A. E. Hanna and M. Tinkham, Phys. Rev. B **44**, 5919 (1991).
[9] J. E. Macdonald, M. Bar Sadan, L. Houben, I. Popov, and U. Banin, Nat. Mater. **9**, 810 (2010).
[10] K. Vinokurov, J. E. Macdonald, and U. Banin, Chem. Mater. **24**, 1822 (2012).
[11] D. Steiner, T. Mokari, U. Banin, and O. Millo, Phys. Rev. Lett. **95**, 056805 (2005).
[12] D. Mocatta, G. Cohen, J. Schattner, O. Millo, E. Rabani, and U. Banin, Science **332**, 77 (2011).
[13] O. Millo, U. Banin, Y. W. Cao, and D. Katz, Nature **400**, 542 (1999).
[14] P. Liljeroth, P. A. Zeijlmans van Emmichoven, S. G. Hickey, H. Weller, B. Grandidier, G. Allan, and D. Vanmaekelbergh, Phys. Rev. Lett. **95**, 086801 (2005).
[15] See Supplemental Material at http://link.aps.org/supplemental/10.1103/PhysRevB.86.085431.
[16] U. Meirav, P. L. McEuen, M. A. Kastner, E. B. Foxman, A. Kumar, and S. J. Wind, Z. Phys. B **85**, 357 (1991).
[17] U. Meirav, M. A. Kastner, and S. J. Wind, Phys. Rev. Lett. **65**, 771 (1990).
[18] C. P. Heij, D. C. Dixon, P. Hadley, and J. E. Mooij, Appl. Phys. Lett. **74**, 1042 (1999).
[19] M. Grobis, A. Wachowiak, R. Yamachika, and M. F. Crommie, Appl. Phys. Lett. **86**, 204102 (2005).
[20] S. Gustavsson, R. Leturcq, B. Simovic, R. Schleser, T. Ihn, P. Studerus, K. Ensslin, D. C. Driscoll, and A. C. Gossard, Phys. Rev. Lett. **96**, 076605 (2006).
[21] C. Rössler, B. Küng, S. Dröscher, T. Choi, T. Ihn, K. Ensslin, and M. Beck, Appl. Phys. Lett. **97**, 152109 (2010).
[22] Y. Meir and N. S. Wingreen, Phys. Rev. Lett. **68**, 2512 (1992).
[23] E. Bonet, M. M. Deshmukh, and D. C. Ralph, Phys. Rev. B **65**, 045317 (2002).
[24] See Supplemental Material at http://link.aps.org/supplemental/10.1103/PhysRevB.86.085431 for the complete theoretical model.
[25] H. Zhang, D. Mautes, and U. Hartmann, Nanotechnology **18**, 065202 (2007).
[26] E. P. A. M. Bakkers, Z. Hens, A. Zunger, A. Franceschetti, L. P. Kouwenhoven, L. Gurevich, and D. Vanmaekelbergh, Nano Lett. **1**, 551 (2001).
[27] U. Banin and O. Millo, Annu. Rev. Phys. Chem. **54**, 465 (2003).